Secondary mineral formation associated with respiration of nontronite, NAu-1 by iron reducing bacteria

S. Erin O'Reilly, Janet Watkins, and Yoko Furukawa[a)]
Naval Research Laboratory, Seafloor Sciences Branch, Stennis Space Center, Mississippi 39529

(Received 10 May 2005; accepted 30 August 2005; published 24 October 2005)

Experimental batch and miscible-flow cultures were studied in order to determine the mechanistic pathways of microbial Fe(III) respiration in ferruginous smectite clay, NAu-1. The primary purpose was to resolve if alteration of smectite and release of Fe precedes microbial respiration. Alteration of NAu-1, represented by the morphological and mineralogical changes, occurred regardless of the extent of microbial Fe(III) reduction in all of our experimental systems, including those that contained heat-killed bacteria and those in which O_2, rather than Fe(III), was the primary terminal electron acceptor. The solid alteration products observed under transmission electron microscopy included poorly crystalline smectite with diffuse electron diffraction signals, discrete grains of Fe-free amorphous aluminosilicate with increased Al/Si ratio, Fe-rich grains, and amorphous Si globules in the immediate vicinity of bacterial cells and extracellular polymeric substances. In reducing systems, Fe was also found as siderite. The small amount of Fe partitioned to the aqueous phase was primarily in the form of dissolved Fe(III) species even in the systems in which Fe(III) was the primary terminal electron acceptor for microbial respiration. From these observations, we conclude that microbial respiration of Fe(III) in our laboratory systems proceeded through the following: (1) alteration of NAu-1 and concurrent release of Fe(III) from the octahedral sheets of NAu-1; and (2) subsequent microbial respiration of Fe(III). © *2005 American Institute of Physics*. [DOI: 10.1063/1.2084787]

INTRODUCTION

Mechanistic pathways of microbial iron reduction in clay minerals are of great interest to sedimentary biogeochemists as Fe(III) minerals are major terminal electron acceptors (TEA) for organic matter (OM) remineralization in a wide range of sedimentary environments.[1–5] The pathways are also of interest to soil scientists: Fe(III) reduction in crystalline clay minerals causes fundamental changes to the physicochemical properties of soil clays such as swellability, exchange capacity, and flocculation properties, affecting their characteristics in agricultural and contaminant dynamics contexts.[6,7]

It has been considered that more Fe(III) is subject to reduction by inorganic reducing agents, such as aqueous sulfides, than to reduction by microbial respiration in typical marine sediments.[8,9] The formation of crystalline iron sulfides such as pyrite in deep sea, margin, and shelf sediments has been reported to be dominated by abiotic reactions between microbially reduced aqueous sulfides and Fe(III) bound to detrital minerals.[10] Recent studies in salt marsh environments, however, highlight the quantitative significance of Fe(III) reduction by microbial respiration in sediments with high reworking rates.[5,11,12] In these environments, more than 50% of the OM remineralization can be attributed to Fe(III) minerals as TEA.[13]

Until recently, microbial Fe(III) reduction in sediments was believed to be limited to the respiration of Fe(III) in poorly crystalline iron (oxy)hydroxides such as nanogoethite and ferrihydrite.[14] However, several laboratory studies have suggested that Fe(III) contained in the octahedral sheets of ferruginous smectite clays could also be available for microbial respiration by dissimilatory iron reducing bacteria (DIRB).[6,15,16] The hypothesis, that DIRB may be able to respire structural Fe(III) in ferruginous clays, then prompted recent studies on interactions between DIRB and ferruginous clay minerals.[17–23]

Despite the abundance of recent experimental studies, the mechanisms of interactions between DIRB and ferruginous clays are not well understood. Past studies of DIRB-Fe oxides interactions have suggested that direct contact between Fe oxide surfaces and bacterial cells is required, or at least highly desirable.[24–28] However, bacterial cells interacting with ferruginous smectite can only be in direct contact with Fe atoms at the sheet edges of or within defect sites of the clay mineral because Fe in ferruginous smectite is predominantly located in the octahedral sheets that are shielded from the surface by the tetrahedral sheets.[29] Thus, if microbial Fe(III) respiration was to proceed via a solid-state transformation of Fe(III) to Fe(II), it would require a solid-state transfer of electrons across tetrahedral sheets. Alternatively, reduction may also occur at the sheet edges where electrons may be transferred along an octahedral sheet to where it is terminated and exposed. Possible mechanisms for such electron transfer processes are still under debate.[30]

Existing studies specific to DIRB-smectite interactions have focused on the relationship between microbial activities and the extent of Fe reduction,[6,21] microbial growth,[20] and changes to the bulk physicochemical properties of clays.[22] Little attention has been given to the mineralogical evolu-

[a)]Author to whom correspondence should be addressed; electronic mail: yoko.furukawa@nrlssc.navy.mil

tions that occur during and as a result of DIRB-clay interactions. A recent study identified some of the secondary minerals recovered at the end of incubations (i.e., biogenic smectite with increased interlayer cations, vivianite).[17] However, the phases reported were not exhaustive, for example, as Al-rich solid phases, expected from the observed nonstoichiometric aqueous release of Si, Al, and Fe, were not shown. In addition, the report was limited to anaerobic systems with or without viable DIRB. More systematic mineralogical descriptions would be desired if mechanistic pathways are to be discussed based on mineralogy. Consequently, the focus of this study is to investigate the alteration of ferruginous smectite in systems with active DIRB-clay interactions with and without O_2 as the TEA, and to discuss mechanistic pathways that yielded the observed secondary mineral assemblages.

LABORATORY EXPERIMENTS

In order to examine the mechanisms of DIRB and ferruginous clay interactions, we conducted two sets of laboratory experiments. The first set (Experiment 1) was a flow-through experiment using a miscible-type flow-through reactor in which the extent of Fe(III) reduction in solids was determined at the end of seven days, and solid phases were investigated using transmission electron microscopy (TEM). The second set (Experiment 2) was a series of batch incubation experiments in which the viability of DIRB and availability of O_2 as the primary TEA were varied. The extent of Fe(III) reduction was determined for each incubation culture, and solid products were analyzed for secondary mineralogy using TEM. In this manuscript, we focus on the link between the extent of microbial Fe(III) reduction and mineralogical changes, and discuss mechanistic pathways that are responsible for the changes.

Materials

Nontronite NAu-1 (Clay Minerals Society Source Clays Repository) is a ferruginous (4.50 mmol Fe g^{-1}) smectite from the Uley Graphite Mine in Australia.[31] It was ground, size-fractioned, and freeze dried prior to use. Only the <0.2 μm fraction was used for the experiments reported here, ensuring $>99\%$ purity.[31] Prior to each experiment, a required amount of size-fractionated NAu-1 was sterilized by microwave radiation, and sterility was confirmed with the lack of bacterial growth in Luria-Bertani (LB) agar after 24 hours.

A minimal culture medium (i.e., M1 medium), adapted from Myers and Nealson,[32] was used in our experiments. This medium has a chemical composition (Table II) that is better defined than other culture media commonly used with *S. oneidensis* such as LB medium. It was specifically developed for the cultivation of *S. oneidensis*,[33] and has been successfully employed by the previous studies of ferruginous clay-*S. oneidensis* incubations.[6,17,21,22] For experiments reported here, M1 was diluted to 25% because full strength media was not necessary for flow studies, which constantly supply fresh media, and batch studies were designed analogous to flow studies.

S. oneidensis bacteria strain MR-1 is a facultative anaerobe capable of dissimilatory iron reduction in anaerobic environments.[32] Prior to each experiment, the bacteria, cultured aerobically in LB media, were diluted into fresh LB media and cultured under continuous 200 rpm shaking at room temperature to a concentration of 1.8×10^8 cells mL^{-1}. Cultures for Experiment 2 (batch systems) were washed twice and resuspended in 25% M1 before the start of each experiment. LB suspensions were used directly when loading Experiment 1 (miscible-flow systems), but the bacteria were washed free of LB using 25% M1 during the experimental set up prior to each run. For runs lacking viable bacteria, the bacterial suspension was heat killed using microwave radiation prior to the start of the experiment. Sterility was confirmed by lack of growth on LB agar. For experiments with no bacterial cells and no associated biomolecules in Experiment 2, sterile, bacteria-free 25% M1 was used.

Experiment 1

In the flow-through experimental run, NAu-1 (200 mg dry weight) and *S. oneidensis* cells were loaded into a 25-mm-diameter plug-flow reactor supported by a 0.2 μm membrane filter (polyethersulfone membrane), and subsequently exposed to a flow of O_2-free 25% M1 media (including 5 mM lactate) at a flow rate of 0.3 ml min^{-1}. Effluent solutions were pooled into separate aliquots every 40 min for analysis. The entire flow system was enclosed in an anaerobic chamber to ensure that Fe(III) in NAu-1 was the only TEA for *S. oneidensis*. After seven days, the reactor was opened, and solid products were stored in an O_2-free environment until later analysis of reduced Fe as described below. Viability of DIRB in the solid products was confirmed by culturing. The aliquots of effluent solutions were analyzed for dissolved metal concentrations using inductively coupled plasma atomic emission spectroscopy (ICP).

Experiment 2

Forty milligrams of NAu-1 was added to sterile polypropylene centrifuge tubes and microwave sterilized. Ten milliliters of 25% M1 with 5 mM lactate (±bacterial suspension) was then added. Anaerobic, live culture systems and a series of control systems were prepared that included the following: (1) anaerobic systems with viable bacteria; (2) anaerobic systems with heat killed bacteria; and (3) aerobic systems with viable bacteria. For each experimental setting, three to four tubes were sacrificed at 4, 24, 48, and 168 h for solid and solution analyses as follows. Each tube was centrifuged at 4500 rpm for 10 min, and 7 ml of the supernatant was removed, filtered, and analyzed for dissolved metal concentrations using ICP and spectrophotometry. After pH analysis with a microelectrode or combination electrode, the remainder of the sample was saved to determine the extent of Fe reduction as described in the following section. Samples for transmission electron microscopy (TEM) analysis were collected and prepared as described in the later section. Time series bacterial population counts for anaerobic batches with viable bacteria were estimated using SYBR Green I fluorescent microscopy[34] using a subsample from each run duration;

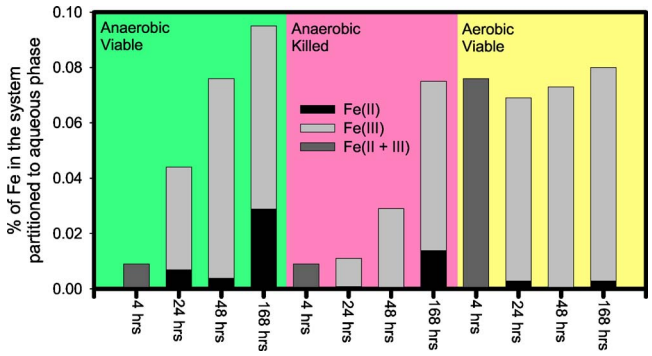

FIG. 1. (Color) The percentage of Fe in each system of Experiment 2 that was partitioned to the aqueous phases. For some of the runs, the Fe(II)/Fe(III) ratio of aqueous Fe were determined by ferrozine assay, and are reported here. Note that the aqueous partitioning of Fe was extremely small (<0.1% of total Fe in the system).

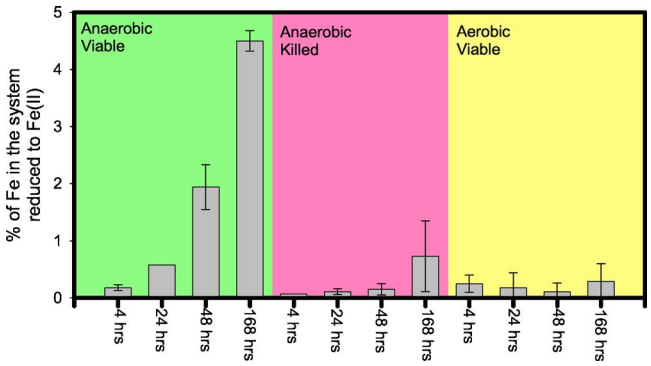

FIG. 2. (Color) The percentage of Fe in each system of Experiment 2 that was in the reduced Fe(II) form. Note that most of the Fe(II) was partitioned into the solid phases. The mean and standard deviation of duplicate runs under each condition are shown.

the counts yielded 1.4×10^8 cells ml^{-1} at time zero and 1.2×10^8, 1.1×10^8, 8.4×10^8, and 1.4×10^8 cells ml^{-1} at 4, 24, 48, and 168 h, respectively. These values indicate that bacteria remained viable for the duration of anaerobic batch experiments inoculated with viable bacteria.

Fe(II) and Fe(III) analysis for solutions

The concentrations of dissolved Fe(II) and Fe(III) species in supernatant solutions from Experiment 2 (i.e., batch experiments) were determined by the ferrozine procedure using the spectrophotometric analytical protocol described by Viollier and co-workers which utilizes dissolved Fe(III) solutions and their reduced products after the addition of hydroxylamine hydrochloride as standards.[35] The interpretation of spectrophotometry readings was conducted according to the updated procedure described by Washington and co-workers.[36] In addition, total dissolved Fe [i.e., aqueous Fe(II)+Fe(III)] concentrations were determined by ICP for the effluent solution aliquots from Experiment 1 (i.e., flow-through experiment) and supernatant solutions from Experiment 2 (i.e., batch experiments). It should be noted that the concentration of total dissolved Fe in each pool of effluent solutions of Experiment 1 (i.e., flow-through experiment) was very small (<2 μmoles l^{-1}] and thus the relative concentrations of dissolved Fe(II) and Fe(III) were not determined with the ferrozine procedure for Experiment 1.

Total Fe(II) analysis

The extent of Fe reduction was determined by the sum of solid-phase Fe(II) (via 60 min 0.5 N HCl extraction followed by the ferrozine assay[17,37]] and Fe(II) in aqueous phase (as determined above). In reality, the quantity of dissolved Fe(II) in aqueous phase was negligible (i.e., <1%] compared to the quantity of solid-phase Fe(II) in all of the reducing systems. It should be noted that crystalline silicates, including NAu-1, do not completely dissolve in 0.5 N HCl, and thus this Fe(II) extraction method through partial digestion is valid only when Fe(II) is exclusively associated with nonsilicates (e.g., carbonates, surface sorbed species) and poorly crystallized clays. However, the method has been shown to fully extract solid-phase Fe(II) resulting from the microbial reduction of ferruginous smectite clays in laboratory cultures similar to our experimental cultures, as a good agreement was previously confirmed between Fe(II) extracted by 0.5 HCl, Fe(II) quantified by the solid-state Mössbauer spectroscopy, and Fe(II) quantified following the whole-clay digestion by HF $+H_2SO_4$.[6]

The percentage of Fe reduced in each sample was determined by the comparison between (A) HCl-extracted Fe(II) plus Fe(II) in the supernatant and (B) total Fe of the starting mixture which includes Fe in NAu-1 (i.e., 4.50 mmol Fe per each gram of NAu-1 as previously reported[31]] and Fe in the 25% M1 media.

For Experiment 1 (i.e., flow-through experiment), solids on the reactor filter paper were dried, weighed, and added to a test tube preloaded with 10 ml of 0.5 N HCl. The test tube was capped and vortexed immediately. All of these steps were conducted inside the anaerobic chamber. One hour after the addition of the solids into the 0.5 N HCl, the test tube was removed from the anaerobic chamber, and an aliquot of the extract solution was analyzed for HCl-extracted Fe(II) using ferrozine assay.[17,37]

After the removal of 7 ml supernatant solution for ICP analysis, each sample from Experiment 2 (i.e., batch experiments) contained 3 ml of solution in addition to the solids. Seventeen milliliters of 0.6 N HCl was added to this mixture for 1 h digestion, followed by the ferrozine assay. The ferrozine assay in this case determined the sum of Fe(II) extracted from solids and Fe(II) that existed in the remaining 3 ml of aqueous phase. Consequently, a correction was made to account for the aqueous Fe(II) removed along with the 7 ml ICP subsample, by using the aqueous Fe(II) concentrations determined by the ferrozine assay.

TEM analysis

Samples were prepared for TEM analysis from Experiment 2 (i.e., batch experiments) as follows. After centrifugation, a 5 μl aliquot of the mixture of aqueous solution and solid suspension was transferred to a BEEM capsule filled with prepared Nanoplast resin using a pipette. Nanoplast is a hydrophilic resin that has been successfully used to prepare aqueous suspensions of organoclay complexes for TEM ultrathin section preparations.[38–41] It has become the embed-

TABLE I. Experimental conditions for batch cultures.

	Initial Conditions						Auqueous phase Fe results						Solid Fe extraction results			Fe reduction	
Sample ID	Description	Run (hrs)	Total NAu-1 in system (g)	Fe(III) (mols) in initial NAu-1	Aqueous culture media (25% M1) (ml)	Fe(total) (mols) in initial aqueous culture media	Total Fe(aq) in media[a] (M)	% Fe in system partitioned to aqueous phase	Fe(II) in media[b] (M)	Fe(II)+ Fe(III) in media[b] (M)	Fe(III) in media by difference (M)	Fe(II) in aqueous media (mols)	Extraction fluid volume[c] (ml)	Fe(II) in extraction fluid (M)	Fe(II) in extraction fluid (mols)	Total reduced Fe(II)[d] (micromols)	% Fe reduction
200	Anoxic Live	4	0.0403	1.81E−04	10	1.35E−08	1.68E−06	0.0					20	1.96E−05	3.92E−07	3.92E−07	0.2
201	Anoxic Live	4	0.0401	1.80E−04	10	1.35E−08	1.45E−06	0.0					20	1.32E−05	2.63E−07	2.63E−07	01
202	Anoxic Live	4	0.0401	1.80E−04	10	1.35E−08	1.51E−06	0.0					20				
203	Anoxic Live	4	0.0402	1.81E−04	10	1.35E−08	1.75E−06	0.0					20				
204	Anoxic Live	24	0.0401	1.80E−04	10	1.35E−08	5.72E−06	0.0	6.00E−07	3.68E−06	3.08E−06	6.00E−09	20	5.19E−05	1.04E−06	1.04E−06	0.6
205	Anoxic Live	24	0.0402	1.81E−04	10	1.35E−08	8.98E−06	0.0					20	5.19E−05	1.04E−06	1.04E−06	0.6
206	Anoxic Live	24	0.0402	1.81E−04	10	1.35E−08	8.44E−06	0.0					20				
207	Anoxic Live	24	0.0400	1.80E−04	10	1.35E−08	8.52E−06	0.0					20				
208	Anoxic Live	48	0.0399	1.80E−04	10	1.35E−08	1.31E−05	0.1	8.00E−07	1.62E−05	1.54E−05	8.00E−09	20	1.49E−04	2.97E−06	2.98E−06	17
209	Anoxic Live	48	0.0402	1.81E−04	10	1.35E−08	1.41E−05	0.1					20	2.00E−04	4.00E−06	4.00E−06	2.2
210	Anoxic Live	48	0.0400	1.80E−04	10	1.35E−08	1.36E−05	0.1					20				
211	Anoxic Live	48	0.0400	1.80E−04	10	1.35E−08	1.37E−05	0.1					20				
212	Anoxic Live	168	0.0400	1.80E−04	10	1.35E−08	1.85E−05	0.1	6.00E−07	1.84E−05	1.78E−05	6.00E−09	20	3.94E−04	7.87E−06	7.888E−06	4.4
213	Anoxic Live	168	0.0403	1.81E−04	10	1.35E−08	2.27E−05	0.1					20	4.20E−04	8.39E−06	8.39E−06	4.6
214	Anoxic Live	168	0.0399	1.80E−04	10	1.35E−08	2.02E−05	0.1					20				
215	Anoxic Live	168	0.0400	1.80E−04	10	1.35E−08	7.10E−06	0.0	7.90E−06	1.35E−05	5.59E−06	7.90E−08	20				
216	Anoxic Killed	4	0.0403	1.81E−04	10	1.35E−08	1.62E−06	0.0					20	6.70E−06	1.34E−07	1.34E−07	0.1
217	Anoxic Killed	4	0.0403	1.81E−04	10	1.35E−08	1.63E−06	0.0					20	6.70E−06	1.34E−07	1.34E−07	0.1
218	Anoxic Killed	4	0.0399	1.80E−04	10	1.35E−08	1.60E−06	0.0					20				
219	Anoxic Killed	24	0.0401	1.80E−04	10	1.35E−08	1.80E−06	0.0	BDL[e]	1.48E−06	1.34E−06	BDL	20	6.70E−06	1.34E−07	1.33E−07	0.1
220	Anoxic Killed	24	0.0402	1.81E−04	10	1.35E−08	1.79E−06	0.0					20	1.32E−05	2.63E−07	2.63E−07	0.1
221	Anoxic Killed	24	0.0403	1.81E−04	10	1.35E−08	1.86E−06	0.0					20				
222	Anoxic Killed	48	0.0402	1.81E−04	10	1.35E−08	2.41E−06	0.0	BDL	1.42E−06	1.42E−06	BDL	20	6.70E−06	1.34E−07	1.34E−07	0.1
223	Anoxic Killed	48	0.0401	1.80E−04	10	1.35E−08	2.51E−06	0.0					20	1.96E−05	3.92E−07	3.92E−07	0.2
224	Anoxic Killed	48	0.0400	1.80E−04	10	1.35E−08	2.47E−06	0.0					20				
225	Anoxic Killed	168	0.0399	1.80E−04	10	1.35E−08	1.33E−05	0.1	3.80E−06	2.01E−05	1.63E−05	3.80E−08	20	1.03E−04	2.07E−06	2.10E−06	1.2
226	Anoxic Killed	168	0.0400	1.80E−04	10	1.35E−08	8.71E−06	0.0					20	2.61E−05	5.21E−07	5.21E−07	0.3
227	Anoxic Killed	168	0.0403	1.81E−04	10	1.35E−08	1.89E−05	0.1					20				
228	Oxic Live	4	0.0401	1.80E−04	10	1.35E−08	1.32E−05	0.1					20	3.25E−05	6.50E−07	6.50E−07	0.4
229	Oxic Live	4	0.0400	1.80E−04	10	1.35E−08	1.20E−05	0.1					20	1.32E−05	2.63E−07	2.63E−07	0.1
230	Oxic Live	4	0.0402	1.81E−04	10	1.35E−08	1.27E−05	0.1					20				
231	Oxic Live	24	0.0400	1.80E−04	10	1.35E−08	1.68E−05	0.1	1.10E−06	1.34E−05	1.23E−05	1.10E−08	20	3.25E−05	6.50E−07	6.58E−07	0.4
232	Oxic Live	24	0.0402	1.81E−04	10	1.35E−08	1.54E−05	0.1	BDL	1.59E−05	1.59E−05	BDL	20	2.50E−07	5.00E−09	5.00E−09	0.0
233	Oxic Live	24	0.0399	1.80E−04	10	1.35E−08	1.56E−05	0.1					20				
234	Oxic Live	48	0.0399	1.80E−04	10	1.35E−08	1.75E−06	0.0					20	2.50E−07	5.00E−09	5.00E−09	0.0
235	Oxic Live	48	0.0401	1.80E−04	10	1.35E−08	1.60E−05	0.1	BDL	1.56E−05	1.56E−05	BDL	20	1.96E−05	3.92E−07	3.92E−07	0.2
236	Oxic Live	48	0.0399	1.80E−04	10	1.35E−08	1.59E−05	0.1					20				
237	Oxic Live	168	0.0399	1.80E−04	10	1.35E−08	1.86E−05	0.1	7.00E−07	1.64E−05	1.57E−05	7.00E−09	20	4.54E−05	9.08E−07	9.13E−07	0.5
238	Oxic Live	168	0.0399	1.80E−04	10	1.35E−08	1.887E−05	0.1					20	6.70E−06	1.34E−07	1.34E−07	0.1
239	Oxic Live	168	0.0401	1.80E−04	10	1.35E−08	1.91E−05	0.1					20				

[a]By ICP.
[b]By ferrozine assay.
[c]Includes 3 ml supernatant and 17 ml 0.6 N HCl.
[d]Sum of Fe(II) in 0.5 N HCl extraction solution and dissolved Fe(II) that was removed when 7 ml supernatant was removed.
[e]Detection limit of 0.4 μM was assumed after Washington *et al.* (Ref. 26).

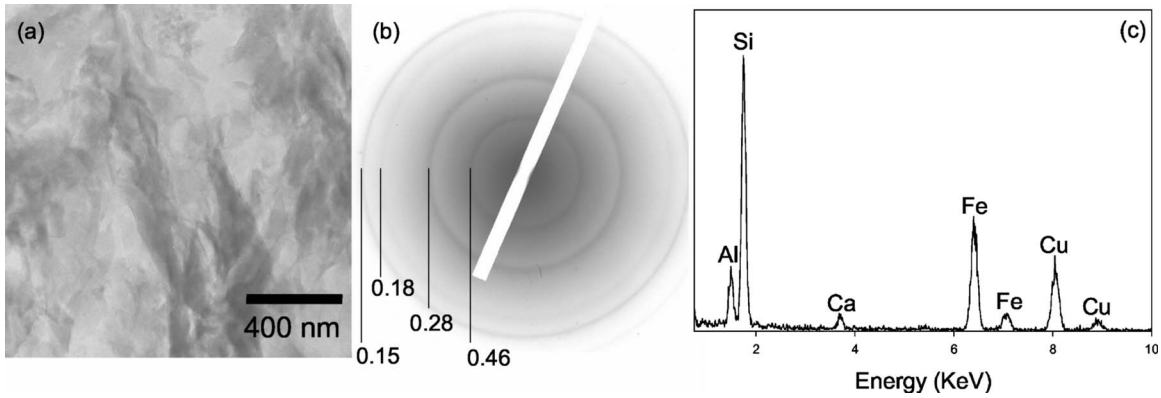

FIG. 3. (a) TEM bright field image of an NAu-1 aggregate suspended in 25% M1 medium. The sample was embedded in hydrophilic resin, which was then cured and sliced into ultrathin sections. (b) SAED pattern of the aggregate, exhibiting well-defined smectite diffraction rings. The corresponding *d*-spacing values (nm) are indicated. (c) EDXS spectrum taken from the aggregate, showing that the aggregate is primarily composed of Si, Al, Fe, and Ca. Note that the Cu signals in this and all other EDXS spectra in this study are from the sample mounting material.

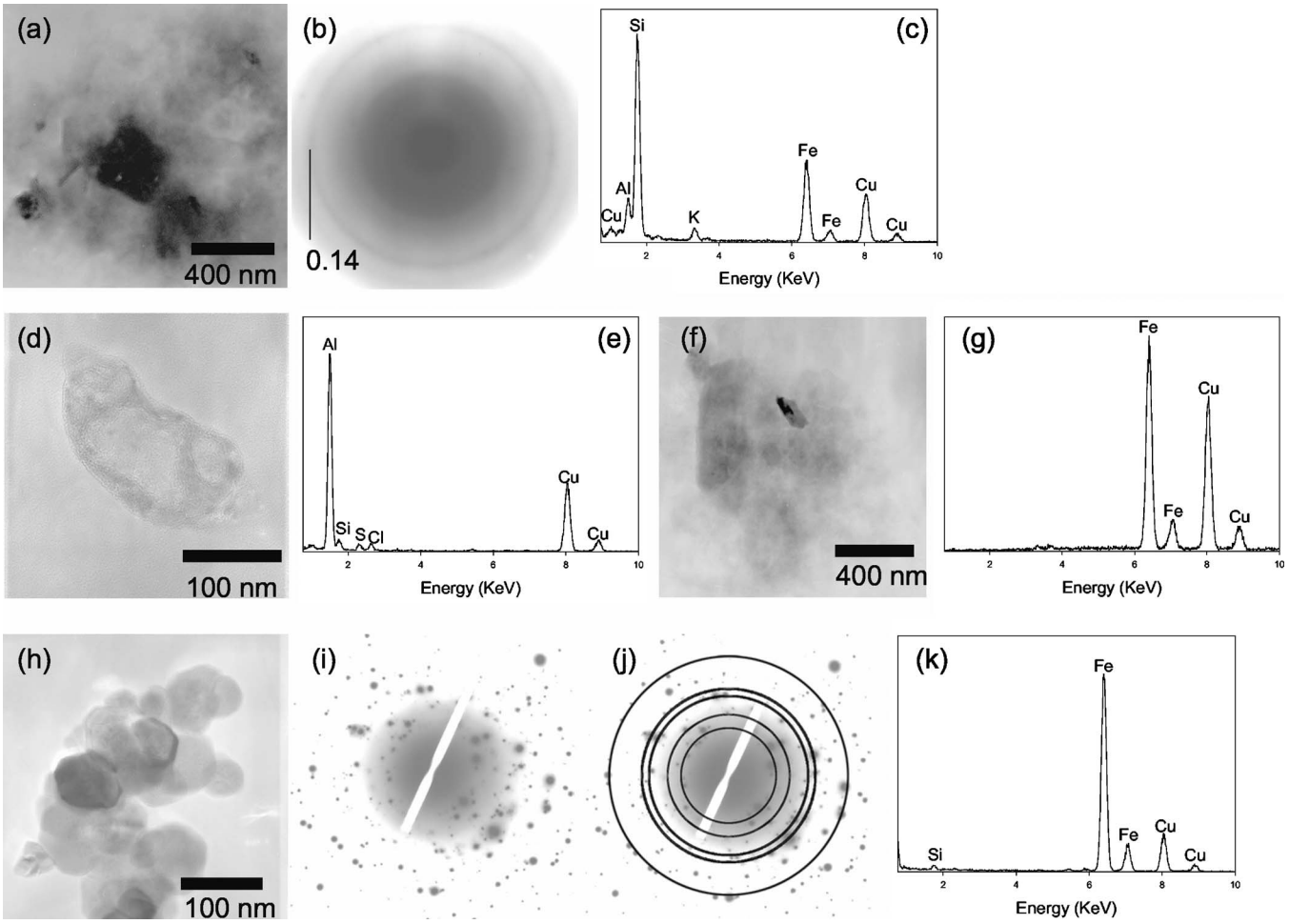

FIG. 4. (a) TEM bright field image of a poorly crystalline aggregate found in the product of 4 hours, anaerobic incubation with viable DIRB. (b) SAED pattern of the aggregate indicates that the particles in this aggregate are poorly crystalline. (c) EDXS spectrum of the aggregate shows that the aggregate is primarily composed of Si, Al, Fe, and K. (d) TEM bright field image of a bacterial cell found in the 24 hours, anaerobic incubation with viable DIRB. (e) EDXS spectrum of the bacterial cell reveals a strong Al signal, indicating that the cell is heavily encrusted with Al, perhaps due to adsorption. (f) TEM bright field image of a particulate organic matter (possibly an EPS) associated with an amorphous solid. (g) EDXS spectrum of the amorphous solid indicates that it is rich in Fe. (h) TEM bright field image of a cluster of nanosized grains with a hexagonal habit found in the 24 hours anaerobic incubation with viable DIRB. (i) SAED pattern for the cluster consists of a series of discrete diffraction spots. (j) The SAED pattern is overlaid with a set of expected powder diffraction rings for siderite (JCPDS Card 8-133). The diffraction rings correspond to the *d*-spacing values (and *hkl* indices) of 3.59 (012), 2.79 (104), 2.13 (113), 1.96 (202), and 1.43 (214). (k) EDXS spectrum from this cluster shows that the cluster is composed predominantly of Fe. Note that the EDXS signals from light elements such as carbon and oxygen are not shown because they appear in the region with high background signals, and also they are abundant in the sample mounting material.

ding material of choice for high-resolution microscopy work in which the structural preservation of organic materials associated with bacterial cells is important. For the preparation of sediments and colloidal suspension in nonmarine, low ionic strength aqueous environments, Nanoplast embedding yields high quality ultrathin sections free of extraction artifacts and salt precipitation with minimal handling disturbance to the structural integrity.[39,42] Nanoplast has also been successfully used for the microstructural preservation of marine organoclay colloids (i.e., marine snow) and microbial communities associated with marine stromatolites without any salt precipitation visible under TEM or confocal microscopy.[43–46] For our samples, we followed the preparation procedure detailed by Leppard and co-workers for the preparation of marine snow.[43] The resin mixture was allowed to slowly replace interstitial water in a 40 °C oven for two days, and subsequently cured at 60 °C for two days. The Nanoplast-embedded sample was ultrathin-sectioned, and examined with JEOL3010 TEM (operated at 300 kV] with Noran energy-dispersive x-ray spectroscopy (EDXS) and selected area electron diffraction (SAED).

RESULTS AND DISCUSSION

Behavior of Fe

Partitioning of Fe between solid and aqueous phases was determined for Experiment 2, along with the ratio of Fe(II) and Fe(III) in the dissolved fraction [Fig. 1 and Table I]. The results indicate that (i) the partitioning of Fe into aqueous phase increased with time during the seven days run in anaerobic viable cultures and anaerobic killed cultures; (ii) aqueous Fe increased immediately within 4 hours in the viable aerobic cultures and held steady for the reminder of seven days run; (iii) the majority of Fe in the dissolved fraction was in the oxidized form [i.e., Fe(III)] even in the anaerobic systems with viable DIRB; (iv) only up to ~0.1% of total Fe was partitioned to the solution whereas ~99.9% of Fe was associated with the solid phases even after seven days (Fig. 1); and (v) net reduction of Fe in the batch systems of Experiment 2 reached 4.5% after seven days in the anaerobic cultures with viable DIRB (Fig. 2).

In the flow-through systems of Experiment 1, very small amounts of Fe were partitioned into the aqueous effluent aliquots during the seven days run, and the cumulative total reached a mere ~0.2% of the original Fe present in the solid starting material, 200 mg of NAu-1 (data not shown).

Net reduction of Fe in the anaerobic, viable flow system of Experiment 1 reached 7.0(±1.0)% of the original Fe present in NAu-1 after seven days. Note this value is from the triplicate analysis of solids recovered from the miscible-flow reactor cell when the experiment was terminated after seven days. The amount of reduced Fe(II) present in the aqueous phase can be considered negligible because the aqueous partitioning of total Fe was very small.

The extent of reduction observed here (i.e., up to ~4.5% in batch systems and ~7% in flow-through system) is less than the numbers reported previously for the microbial reduction of SWa-1 nontronite (i.e., ~30%–45%][6,17,21,22] which is crystallographically different from NAu-1: the octahedral sheets of SWa-1 contain more Al and Mg and less Fe(III) than those of NAu-1.[29]

The behavior of Fe alone might suggest a solid-state transformation of NAu-1 to a clay that contains Fe(II) rather than Fe(III), as very little Fe is detected in the aqueous phase. However, the TEM analysis reveals extensive solid phase alterations as discussed in the next section.

Identification of solid products

Figures 3(a)–3(c) shows a TEM image of an unaltered aggregate of NAu-1 [Fig. 3(a)], the associated SAED pattern [Fig. 3(b)], and EDXS profile [Fig. 3(c)]. The TEM image shows an aggregate of clay particles with wavy appearances typical of smectitic clays.[47] The SAED pattern exhibits a typical smectite electron diffraction pattern. The EDXS spectrum indicates abundant Si along with Al, Fe, and Ca.

Figures 4(a)–4(c) is a product of NAu-1 alteration after 4 hours in the batch anaerobic live culture. The particles appear very poorly crystalline in the bright-field image [Fig. 4(a)], which is corroborated by the SAED pattern [Fig. 4(b)] which is much more diffused than the diffractions of original NAu-1 [i.e., Fig. 3(b)]. The EDXS spectrum indicates its elemental composition to be still similar to the original NAu-1 in terms of Al, Si, and Fe. The Ca peak present in original NAu-1 has been replaced by the K peak, suggesting cation exchange with the aqueous medium which contains more K than Ca (see Table II). The occurrence of poorly

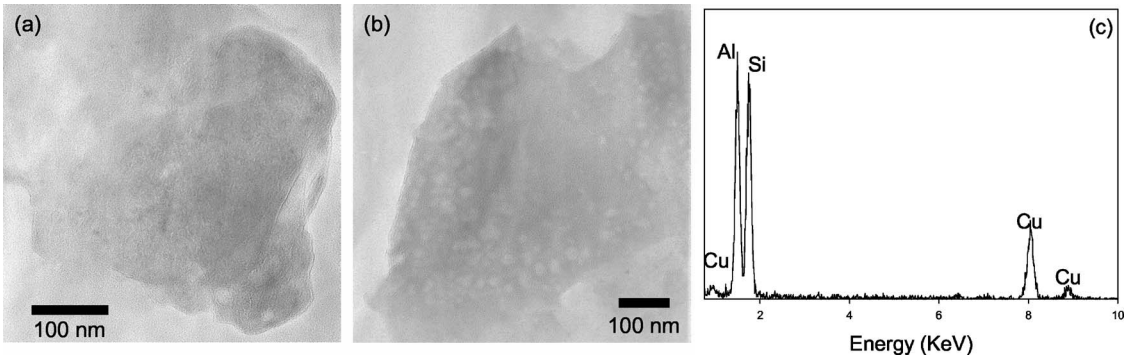

FIG. 5. (a) and (b) TEM bright field images of the discrete particles of amorphous aluminosilicate found in the 7 days, anaerobic incubation in the flow-through system with viable DIRB. (c) The EDXS spectra of these particles indicate that they are primarily composed of Al and Si, while other cations are undetected.

TABLE II. Composition of full-strength M1 medium [after Myers and Nealson (Ref. 32) and Kostka and Nealson (Ref. 33)].

Component	Concentration
Lactate	20 mM
$(NH_4)_2SO_4$	9.0 mM
K_2HPO_4	5.7 mM
KH_2PO_4	3.3 mM
$NaHCO_3$	2.0 mM
$MgSO_4$	1.01 mM
$CaCl_2$	0.485 mM
Na_2EDTA	67.2 μM
H_3BO_3	56.6 μM
NaCl	10.0 μM
$FeSO_4$	5.4 μM
$CoSO_4$	5.0 μM
$Ni(NH_4)_2(SO_4)_2$	5.0 μM
Na_2MoO_4	3.87 μM
Na_2SeO_4	1.5 μM
$MnSO_4$	1.26 μM
$ZnSO_4$	1.04 μM
$CuSO_4$	0.2 μM
Arginine	20 mg L^{-1}
Glutamate	20 mg L^{-1}
Serine	20 mg L^{-1}

crystalline smectite was widespread in the samples from 4 hours anaerobic live incubations whereas the extent of Fe reduction in those samples was only 0.1%–0.2% (see Fig. 2 and Table I). This suggests that NAu-1 alteration precedes microbial Fe reduction. The 24 h anaerobic live culture also contained bacterial cells in intimate association with Al [Figs. 4(d) and 4(e)]. Amorphous, Fe-rich precipitates were also found to be associated with particulate organic matter [likely extracellular polymer substances (EPS)] in the 4 h incubation product of an anaerobic, viable culture [Fig. 4(f)]. Trivalent cations such as Al and Fe(III) are electrostatically attracted to negatively charged bacteria surfaces and EPS,[48] thus Al and Fe ions released due to NAu-1 alteration would be expected to become associated with bacterial cells and EPS, as observed in these images. In addition, siderite with the morphology similar to those formed by the DIRB reduction of amorphous ferric hydroxides[49] was found in the anaerobic, live culture after 24 h of incubation [Figs. 4(h)–4(k)].

After the seven days of anaerobic, live, flow-through experiments in which Fe(III) from NAu-1 was the only TEA, the products exhibited evidence of further alterations. Small, discrete domains of amorphous particles rich in Al and Si were observed [Figs. 5(a) and 5(b)]. The amorphous nature of these particles was confirmed by SAED (data not shown). EDXS analyses of these particles revealed that the relative ratio of Al to Si is greater than that of the original NAu-1 shown in Fig. 3(c). Some of the elements abundant in the original NAu-1 in octahedral sites as well as in interlayer spaces, namely Fe and Ca, are absent in these amorphous aluminosilicate phases. The Al/Si ratio of these particles and the absence of Fe and Ca make the chemical composition of these particles closer to that of kaolinite group clays (e.g., kaolinite and halloysite) than that of NAu-1. Transformation of low Al/Si clays to poorly ordered aluminosilicates with near-unity Al/Si ratio in the immediate vicinity of bacterial cells has been previously reported from weathered pyroclastic deposits,[50] in experimental incubations of volcanic ash,[51] in lake sediments enriched with metal contaminants,[52] and in river sediments in association with fresh water biofilms.[53–55] These previous authors have attributed the transformation to the three step process: (1) dissolution of primary minerals; (2) subsequent interaction between bacterial cell surfaces and dissolved cations; and (3) precipitation of poorly ordered aluminosilicate phases.

Alteration products were also found in aerobic batch systems in which DIRB respired O_2 rather than Fe(III) from NAu-1. After seven days of aerobic, live, batch incubation, the samples contained poorly crystalline smectitic clays with Si, Al, and Fe [Figs. 6(a) and 6(b)]. Cation exchange in the aerobic sample was not as extensive as the cation exchange that occurred in the anaerobic batch sample, as the Ca peak was still visible [e.g., comparison between Figs. 4(c) and 6(b)]. The same seven days aerobic, live, batch incubation also included amorphous aluminosilicates with increased Al/Si ratio similar to the ones shown in Fig. 5.

In addition to the above phases, amorphous Si globules with ~50 nm diameter in close association with bacterial cells and the EPS were found in all systems that contained either viable or killed bacterial cells [Figs. 7(a) and 7(b)]. This is in agreement with previous studies that found cell surfaces or EPS to be the site of silica polymerization.[56,57]

In anaerobic batch systems with killed DIRB, amorphous Fe precipitates were found in close association with amorphous Si globules [Figs. 8(a) and 8(b)]. These systems contained nonviable cells of *S. oneidensis* along with any

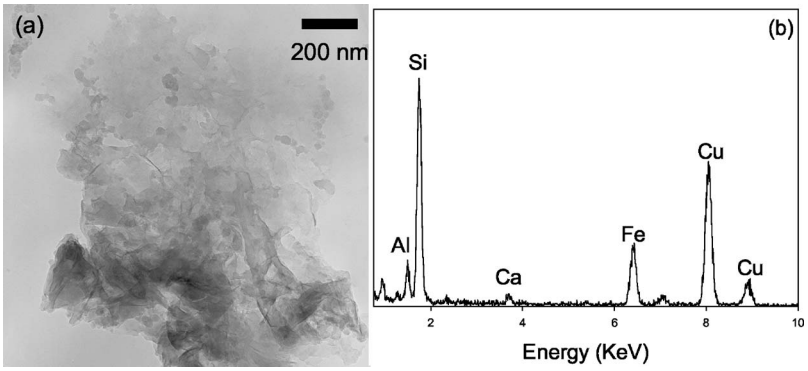

FIG. 6. (a) TEM bright field image of a cluster of poorly crystalline clay mineral particles found in the 7 days aerobic incubation. (b) EDXS spectrum of the aggregate shows that the elemental composition of these poorly crystalline particles is similar to that of NAu-1.

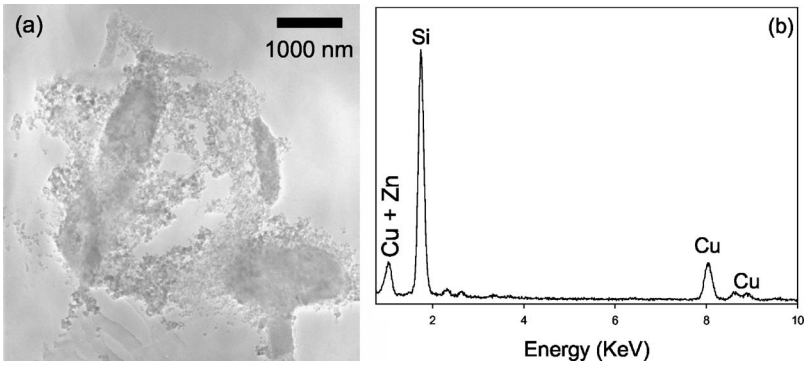

FIG. 7. (a) In all systems with either viable or killed DIRB, regardless of the O_2 concentrations, we found small (~50 nm) globules of amorphous Si encrusting bacterial cells and EPS, as shown in this TEM bright field image. (b) EDXS spectrum shows that the amorphous globules are rich in Si. The Zn signal is from the sample mounting material.

biomolecules and EPS produced by the bacteria before the heat treatment.

In order to maintain mass balance, the secondary formation of Fe-poor phases such as those seen in Figs. 5(a), 5(b), and 7(a) must be accompanied by the formation of Fe-rich phases such as those found in Figs. 4(f), 4(h), and 8(a). In reducing (i.e., anaerobic live culture) systems, Fe(II) minerals such as siderite [e.g., Fig. 4(f)] are expected to precipitate. In the absence of microbial Fe(III) reduction, or if the rate of microbial Fe(III) reduction is less than the rate of NAu-1 alteration, Fe(III) may be incorporated into poorly crystalline, high-surface area Fe(III) precipitates, or it may be adsorbed onto other solid phases or negatively charged bacterial cells and EPS.[58] The high reactivity of poorly crystalline Fe(III) precipitates with a large specific surface area toward microbial respiration has been quantitatively recognized.[59] In addition, a small, but finite quantity of dissolved Fe(III) was detected in all of our experimental batch systems (Fig. 1). Thus, it is possible that Fe(III) incorporated into secondary phases, adsorbed onto the surfaces of secondary phases or bacterial cells, or dissolved Fe(III) species, rather than Fe(III) in the octahedral sheets of original NAu-1, is the primary TEA in our experimental systems.

These observations suggest that a portion of original NAu-1 present in each system, regardless of the O_2 content or biological conditions, undergoes alteration and transforms to poorly crystalline smectite as well as authigenic phases in the aqueous medium used in our experimental systems. Poorly crystalline smectite was found in all systems (i.e., anaerobic live, anaerobic killed, and aerobic live). Amorphous aluminosilicates with increased A/Si ratio were found in the anaerobic, live flow-through culture as well as in the seven days incubation of aerobic live culture. In reducing systems (i.e., anaerobic live cultures), siderite was also found. These observations indicate that microbial Fe(III) respiration is not a prerequisite for the NAu-1 alteration. NAu-1 alteration was observed in all systems including those in which *S. oneidensis* respired O_2, and those in which no viable cells were present. The secondary phases identified by TEM are summarized in Table III.

Coupling between NAu-1 alteration and Fe reduction

Brief (4 hours–7 days) incubations with viable as well as killed bacteria, with or without O_2 as the primary TEA, resulted in clay aggregates that are much less crystalline than the original NAu-1. Secondary mineral phases such as amorphous aluminosilicates with increased Al/Si ratio, and amorphous Si globules in close association with bacterial cells and EPS, were found in our experimental systems regardless of the availability of O_2 as a TEA or the extent of microbial Fe(III) reduction. Meanwhile, although in small quantities, dissolved Fe(III) species were detected in all systems including the reducing systems (Fig. 1). These observations lead us to conclude that microbial Fe(III) reduction occurred after NAu-1 alteration or secondary mineral formation in our experimental systems.

In other words, these observations suggest that microbial reduction is not primarily of Fe(III) within the octahedral sheets of original NAu-1, but of Fe(III) that is no longer a part of the original, well-crystallized NAu-1. It can be speculated that Fe(III) that is no longer associated with the octahedral sheets of well-crystallized NAu-1 would have been more readily available for microbial reduction than Fe(III) in the original NAu-1. In anaerobic systems with viable bacteria, these Fe(III) would be respired by DIRB and transformed

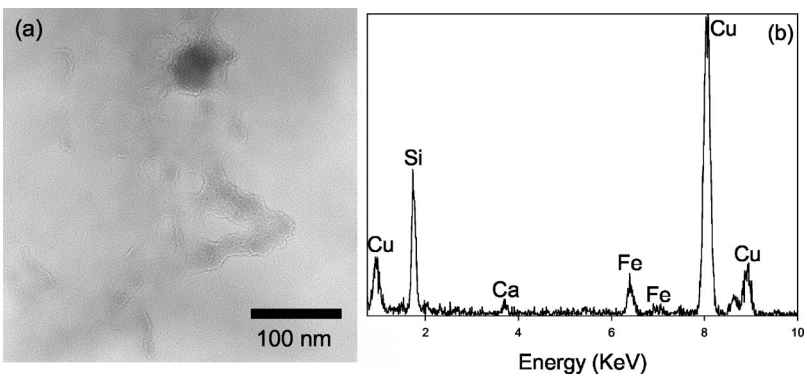

FIG. 8. (a) TEM bright field image of the amorphous Fe precipitate (~50 nm dark grain near the top) associated with chained globules of amorphous Si found in the 7 days anaerobic system with killed DIRB. (b) EDXS spectrum indicates that this assemblage is rich is Fe and Si, along with a small amount of Ca.

TABLE III. Summary of experimental products.

	Flow-through Anaerobic Viable DIRB 7 days	Batch Anaerobic Viable DIRB 4 hours	Batch Anaerobic Viable DIRB 7 days	Batch Anaerobic Killed DIRB 7 days	Batch Aerobic Viable DIRB 7 days
Primary TEA	Fe(III)	Fe(III)	Fe(III)	N/A	O_2
Extent of Fe reduction	7% ± 1%	0.1%–0.2%	4.4%–4.6%	0.3–1.2%	0.1–0.5%
Phases present					
Poorly crystalline smectite	Not found	Yes	Yes	Yes	Yes
Amorphous aluminosilicate with increased Al/Si	Yes	Not found	Not found	Not found	Yes
Amorphous Si	Yes	Yes	Yes	Yes	Yes

to Fe(II). The majority of Fe(II) would then partition into solid phases as Fe(II) minerals and as adsorbed species on EPS and bacterial cells, since little dissolved Fe(II) was detected in the experimental systems.

In summary, microbial reduction of NAu-1 in our laboratory systems proceeded through (1) alteration of NAu-1 to poorly crystalline clays, as well as to Fe-poor aluminosilicates which are mass-balanced by the formation of Fe(III) precipitates or dissolved Fe(III) species; and (2) subsequent microbial respiration of Fe(III) that is not associated with the octahedral sheets of well-crystallized NAu-1. With or without the presence of microbial Fe(III) reduction, the alteration continued to yield such secondary phases as amorphous aluminosilicates with increased Al/Si ratio, amorphous Si globules in close association with bacterial cells and EPS, and amorphous Fe precipitates. Our laboratory study suggests that, in nature, microbial respiration of Fe(III) in clay minerals of anaerobic soils and sediments is initiated by the alteration of clay minerals followed by microbial respiration of Fe(III) that is no longer in the octahedral sheets of well-crystallized clays. This suggested mechanism would make the transfer of electrons through tetrahedral layers of well crystallized smectite unnecessary.

ACKNOWLEDGMENTS

This study was funded by ONR/NRL Core 6.1 funding (PE#0601153N). One of the authors (S.E.O) was supported through the National Research Council at NRL. ICP analysis was conducted by J. Kolberg at Applied Geo Technologies, Inc. (Stennis Space Center, Mississippi). NRL Electron Microscopy Facility (Stennis Space Center, Mississippi) provided support for the TEM analysis. The authors would like to thank S. Newell for assistance with the SYBR Green fluorescence bacterial counting. NRL Contribution No. JA/7430-04-15.

[1]P. N. Froelich, G. P. Klinkhammer, M. L. Bender *et al.*, Geochim. Cosmochim. Acta **43**(7), 1075 (1979).
[2]D. E. Canfield, B. B. Jorgensen, H. Fossing *et al.*, Mar. Geol. **113**(1-2), 27 (1993).
[3]E. E. Roden and R. G. Wetzel, Limnol. Oceanogr. **41**(8), 1733 (1996).
[4]B. Thamdrup and D. E. Canfield, Limnol. Oceanogr. **41**, 1629 (1996).
[5]J. E. Kostka, B. Gribsholt, E. Petrie *et al.*, Limnol. Oceanogr. **47**(1), 230 (2002).
[6]J. E. Kostka, J. W. Stucki, K. H. Nealson *et al.*, Clays Clay Miner. **44**(4), 522 (1996).
[7]J. Kim, Y. Furukawa, H. L. Dong *et al.*, Clays Clay Miner. (in press).
[8]D. E. Canfield, Geochim. Cosmochim. Acta **53**(3), 619 (1989).
[9]D. E. Canfield, B. Thamdrup, and J. W. Hansen, Geochim. Cosmochim. Acta **57**(16), 3867 (1993).
[10]R. Raiswell and D. E. Canfield, Am. J. Sci. **298**(3), 219 (1998).
[11]K. L. Lowe, T. J. Dichristina, A. N. Roychoudhury *et al.*, Geomicrobiol. J. **17**(2), 163 (2000).
[12]C. M. Koretsky, C. M. Moore, K. L. Lowe *et al.*, Biogeochemistry **64**(2), 179 (2003).
[13]Y. Furukawa, A. C. Smith, J. E. Kostka *et al.*, Limnol. Oceanogr. **49**(6), 2058 (2004).
[14]C. van der Zee, D. R. Roberts, D. G. Rancourt *et al.*, Geology **31**(11), 993 (2003).
[15]J. Wu, C. B. Roth, and P. F. Low, Soil Sci. Soc. Am. J. **52**(1), 295 (1988).
[16]J. W. Stucki, P. Komadel, and H. T. Wilkinson, Soil Sci. Soc. Am. J. **51**(6), 1663 (1987).
[17]H. L. Dong, J. E. Kostka, and J. Kim, Clays Clay Miner. **51**(5), 502 (2003).
[18]J. W. Kim, Y. Furukawa, T. L. Daulton *et al.*, Clays Clay Miner. **51**(4), 382 (2003).
[19]H. L. Dong, R. K. Kukkadapu, J. K. Fredrickson *et al.*, Environ. Sci. Technol. **37**(7), 1268 (2003).
[20]J. E. Kostka, D. D. Dalton, H. Skelton *et al.*, Appl. Environ. Microbiol. **68**(12), 6256 (2002).
[21]J. E. Kostka, E. Haefele, R. Viehweger *et al.*, Environ. Sci. Technol. **33**(18), 3127 (1999).
[22]J. E. Kostka, J. Wu, K. H. Nealson *et al.*, Geochim. Cosmochim. Acta **63**(22), 3705 (1999).
[23]J. Kim, H. L. Dong, J. Seabaugh *et al.*, Science **303**(5659), 830 (2004).
[24]D. R. Lovley, D. E. Holmes, and K. P. Nevin, Adv. Microb. Physiol. **49**, 219 (2004).
[25]Y. S. Luu and J. A. Ramsay, World J. Microbiol. Biotechnol. **19**(2), 215 (2003).
[26]K. P. Nevin and D. R. Lovley, Geomicrobiol. J. **19**(2), 141 (2002).
[27]J. F. Heidelberg, I. T. Paulsen, K. E. Nelson *et al.*, Nat. Biotechnol. **20**(11), 1118 (2002).
[28]C. R. Myers and J. M. Myers, J. Bacteriol. **174**(11), 3429 (1992).
[29]W. P. Gates, P. G. Slade, A. Manceau *et al.*, Clays Clay Miner. **50**(2), 223 (2002).
[30]K. M. Rosso and E. S. Ilton, J. Chem. Phys. **119**(17), 9207 (2003).
[31]J. L. Keeling, M. D. Raven, and W. P. Gates, Clays Clay Miner. **48**(5), 537 (2000).
[32]C. R. Myers and K. H. Nealson, Science **240**, 1319 (1988).
[33]J. E. Kostka and K. H. Nealson, in *Techniques in Microbial Ecology*, edited by R. S. Burlage (Oxford University Press, Oxford, 1998), p. 58.
[34]J. Skeidsvoll and P. M. Ueland, Anal. Biochem. **231**(2), 359 (1995).
[35]E. Viollier, P. W. Inglett, K. Hunter *et al.*, Appl. Geochem. **15**(6), 785 (2000).
[36]J. W. Washington, D. M. Endale, L. P. Samarkina *et al.*, Geochim. Cosmochim. Acta **68**(23), 4831 (2004).

[37]J. E. Kostka and K. H. Nealson, Environ. Sci. Technol. **29**(10), 2535 (1995).
[38]C. Mondi, K. Leifer, D. Mavrocordatos *et al.*, J. Microsc. (Paris) **207**, 180 (2002).
[39]D. Perret, G. G. Leppard, M. Muller *et al.*, Water Res. **25**(11), 1333 (1991).
[40]K. J. Wilkinson, E. Balnois, G. G. Leppard *et al.*, Colloids Surf., A **155**(2-3), 287 (1999).
[41]S. M. Webb, G. G. Leppard, and J. F. Gaillard, Environ. Sci. Technol. **34**(10), 1926 (2000).
[42]C. H. Swartz, A. L. Ulery, and P. M. Gschwend, Geochim. Cosmochim. Acta **61**(4), 707 (1997).
[43]G. G. Leppard, A. Heissenberger, and G. J. Herndl, Mar. Ecol.: Prog. Ser. **135**(1–3), 289 (1996).
[44]A. Heissenberger, G. G. Leppard, and G. J. Herndl, Mar. Ecol.: Prog. Ser. **135**(1–3), 299 (1996).
[45]A. W. Decho and T. Kawaguchi, BioTechniques **27**(6), 1246 (1999).
[46]T. Kawaguchi and A. W. Decho, Marine Biotechnology 4(2), 127 (2002).
[47]R. H. Bennett, N. R. O'Brien, and M. H. Hulbert, in *Microstructure of Fine-Grained Sediments*, edited by R. H. Bennett, W. R. Bryant, and M. H. Hulbert (Springer-Verlag, New York, 1990), p. 5.
[48]J. B. Fein, C. J. Daughney, N. Yee *et al.*, Geochim. Cosmochim. Acta **61**(16), 3319 (1997).
[49]J. K. Fredrickson, J. M. Zachara, D. W. Kennedy *et al.*, Geochim. Cosmochim. Acta **62**(19-20), 3239 (1998).
[50]M. Kawano and K. Tomita, Clays Clay Miner. **50**(1), 99 (2002).
[51]M. Kawano and K. Tomita, Am. Mineral. **86**(4), 400 (2001).
[52]F. G. Ferris, W. S. Fyfe, and T. J. Beveridge, Chem. Geol. **63**(3-4), 225 (1987).
[53]K. O. Konhauser, Earth-Sci. Rev. **43**(3-4), 91 (1998).
[54]K. O. Konhauser, S. Schultzelam, F. G. Ferris *et al.*, Appl. Environ. Microbiol. **60**(2), 549 (1994).
[55]K. O. Konhauser, W. S. Fyfe, F. G. Ferris *et al.*, Geology **21**(12), 1103 (1993).
[56]N. Yee, V. R. Phoenix, K. O. Konhauser *et al.*, Chem. Geol. **199**(1-2), 83 (2003).
[57]L. G. Benning, V. R. Phoenix, N. Yee *et al.*, Geochim. Cosmochim. Acta **68**(4), 729 (2004).
[58]S. Glasauer, S. Langley, and T. J. Beveridge, Appl. Environ. Microbiol. **67**(12), 5544 (2001).
[59]E. E. Roden, Environ. Sci. Technol. **37**(7), 1319 (2003).